LOW ANGLE DIRECTION OF ARRIVAL ESTIMATION BY TIME REVERSAL

Xiaolu Zeng[†]*, Minglei Yang*[†]*, Baixiao Chen*[†]*, Yuanwei Jin*[⋆]

[†] National Lab. of Radar Signal Processing, Xidian University, Xi'an, Shaanxi 710071, China
[⋆] Department of Engineering and Aviation Sciences, University of Maryland Eastern Shore, MD 21853, USA

ABSTRACT

In a low angle target parameter estimation scenario, the backscattered signals from targets are distorted by clutter and multipath, which degrades the performance of direction-of-arrival (DOA) estimator significantly. This paper presents a novel method using time reversal (TR) technique and coherent signal-subspace method (CSM) for DOA estimation in a low angle scenario. The TR method exploits target information contained in the return echoes due to multipath and adaptively adjusts TR probing waveforms to increase the signal-to-noise ratio (SNR). Furthermore, CSM is adopted to focus the energy of the multipath signal in a predefined subspace so as to exploit the full time-bandwidth product of the target source. We analyze the performance of the proposed new DOA algorithm. Numerical simulations demonstrate its superior performance compared with the conventional DOA estimators.

***Index Terms*—** Direction-of-arrival (DOA), low-angle scenario, time reversal (TR) technique.

1. INTRODUCTION

Direction-of-arrival (DOA) estimation plays an important role in array signal processing with wide applications in communication, sonar and radar systems [1]. Generally, DOA estimators are based on the direct-path-only propagation observations, in which multipaths are either ignored or considered detrimental to the performance of the corresponding DOA estimation. However, most of these methods will not work well or even fail for low-angle targets in that strong and rich scattering multipaths make it difficult to extract the target useful information accurately from measurement data, thus, reducing DOA estimation accuracy in radar systems. A natural question rises as what can be gained if we exploit the additional information contained in multipaths. Recently Time Reversal (TR) provides a relatively simple methodology that enables constructive utilization of multipaths to adjust the transmitted waveform to the propagation channel so as to mitigate effects of multipath distortions [2, 3, 4, 5].

This work is supported by National Natural Science Foundation of China (61571344).

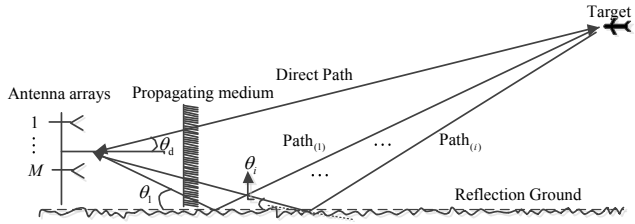

Fig. 1. Geometry of reflection for the TR Localization estimator.

In this paper, we consider a new DOA estimator named time reversal *focusing* spatial smoothing MUSIC (TRF-SSMUSIC) in which the TR technique is adopted to treat the multipath effect positively. Differing from the conventional DOA estimators, the proposed TR estimator adopts an extra TR setup in which case the received backscatter signals from the target is time-reversed and re-transmitted to probe the target once again. The subsequent backscattered signals are then used in our algorithm for DOA estimation. By using TR technique, the TR probing waveform can inherently match the propagation channel and refocus at the original source location to increase the signal-to-noise ratio (SNR) [6]. Considering that the time reversed signal is typically a wide band signal in a DOA estimation problem, we utilize the coherent signal subspace method (CSM) [7] in order to compress the energy of the time reversed signal in a pre-defined space so as to exploit the full time-bandwdith product of the target source and to cope with the coherent wavefronts, thereby, resulting in a better DOA estimation performance compared with the conventional DOA estimators. Therefore, the contribution of the paper is two-fold. First, we develop a new DOA estimator by combining the TR method and the CSM method to address the challenging low-angle target DOA estimation. Second, we conduct numerical simulations to demonstrate the superior performance of the proposed algorithm compared with conventional benchmarking algorithms.

2. SIGNAL MODEL

In this section, we introduce the signal model based on the DOA estimation setup in Fig. 1. Assume the target and sensor arrays are far enough, thus, a far field approximation

holds. The probing signal is supposed to be a known complex bandpass signal $f(t)e^{jw_c t}$ (w_c denotes the angular carrier frequency). Then, the backscatter signal (it is named Forward-Echo to be different from TR-Echo used later) recorded by the kth element of the array after down conversion to baseband and sampling can be expressed as [3, 4, 8]:

$$r_k(t) = \sum_{p=1}^{P} \mathrm{X}_p f(t - \tau_{(p,1)} - \delta_{(k,p)}) + v_k(t), \quad (1)$$

where P, X_p, $\tau_{(p,1)}$, $\delta_{(k,p)}$ and $v_k(t)$ denote the number of paths, attenuation vector, reference delay via path p, interelement delay with path p in excess of $\tau_{(p,1)}$ of element k and noise factor, respectively. Here we assume that the target is stationary or moving with a relatively slow velocity so that the Doppler frequency can be omitted. In the frequency domain, (1) can be written as

$$R_k(\omega) = \sum_{p=1}^{P} \mathrm{X}_p \mathrm{F}(\omega) e^{-j\omega\tau_{(p,1)}} e^{-j\omega\delta_{(k,p)}} + \mathrm{V}_k(\omega). \quad (2)$$

Considering all of the M elements of the array and using (1), Forward-Echo $\mathbf{y}(t)$ can be given by

$$\mathbf{y}(t) = [r_1(t), r_2(t), \cdots, r_k(t), \cdots, r_M(t)]^T. \quad (3)$$

Then the frequency form $\mathbf{y}(\omega)$ can be expressed as

$$\begin{aligned} \mathbf{y}(\omega) &= [R_1(\omega), R_2(\omega), \cdots, R_k(\omega), \cdots, R_M(\omega)]^T \\ &= \mathbf{A}(\boldsymbol{\Theta}) \mathbf{X} \gamma(\omega) \mathrm{F}(\omega) + \mathbf{V}(\omega). \end{aligned} \quad (4)$$

In (4), $\mathbf{A}(\boldsymbol{\Theta})$ is the steering vector matrix given by

$$\begin{aligned} &\mathbf{a}(\theta_p) = [1, \cdots, e^{-j\Omega_k \sin\theta_p}, e^{-j\Omega_{P-1}\sin\theta_p}]^T \\ &\mathbf{A}(\boldsymbol{\Theta}) = [\mathbf{a}(\theta_1), \cdots, \mathbf{a}(\theta_P)], \text{with } \Omega_k = k\omega d/c, \end{aligned} \quad (5)$$

where $\theta_p (p = 1, 2, \cdots, P)$ denotes the angle of the multipath p. $\mathbf{X}$ is the attenuation matrix given by $\mathbf{X} = \mathrm{diag}[\mathrm{X}_1, \cdots, \mathrm{X}_P]$, and $\gamma(\omega) = [e^{-j\omega\tau_{(1,1)}}, \cdots, e^{-j\omega\tau_{(P,1)}}]^T$ representing the reference delay vector. $\mathrm{V}(\omega)$ is the noise vector constructed by $\mathbf{V}(\omega) = [\mathbf{V}_1(\omega), \cdots, \mathbf{V}_M(\omega)]^T$. The operation diag[X] represents a square matrix with elements of X on the main diagonal.

Now we derive the TR-Echo from Forward-Echo presented in (4). Firstly, we review the TR technique briefly. The Forward-Echo (i.e., $\mathbf{y}(\omega)$) is digitized, energy normalized, time-reversed (equivalent to phase conjugation in the frequency domain), and retransmitted to the propagating medium and then backscattered to the ULA sensors again. Note that the propagation environment is supposed to be the same as that in the forward probing step and the reciprocity condition holds. Then, we can get observations in the TR probing step called TR-Echo $\mathbf{y}_{TR}(\omega)$ on the base of (4).

$$\mathbf{y}_{TR}(\omega) = \sum_{m=1}^{M} \mathbf{A}(\boldsymbol{\Theta}) \mathbf{X} \gamma(\omega) \mathbf{z}_m(\omega) + \zeta(\omega), \quad (6)$$

where $\mathbf{z}_m(\omega)$ refers to the mth entry of $\mathbf{z}(\omega)$ while vector $\mathbf{z}(\omega) = g\mathbf{y}^*(\omega)$ denotes the TR probing signal. $\zeta(\omega)$ denotes the noise brought in by the TR probing process and g is the energy normalization factor which can be computed by

$$g = \sqrt{(\|\mathrm{F}(\omega)\|^2)/(\|\mathbf{y}(\omega)\|^2)}, \quad (7)$$

Similar to (4), (6) can be expressed in the matrix format as

$$\mathbf{y}_{TR}(\omega) = \mathbf{A}_{TR}(\boldsymbol{\Theta}) \mathbf{X}_{TR} \boldsymbol{\Gamma}_{TR}(\omega) \mathbf{Z}_{TR}(\omega) + \zeta(\omega). \quad (8)$$

In (8), the block matrix $\mathbf{A}_{TR}(\boldsymbol{\Theta})$ is of order $(M \times MP)$, while $\mathbf{X}_{TR}$ is a square matrix with dimensions of $(MP \times MP)$. Symbol $\mathbf{1}_M$ refers to a row vector of dimension M with all entries equal to 1. Specific meanings of them are defined as follows

$$\begin{aligned} &\mathbf{A}_{TR}(\boldsymbol{\Theta}) = [\mathbf{A}(\boldsymbol{\Theta}) | \mathbf{A}(\boldsymbol{\Theta}) | \cdots | \mathbf{A}(\boldsymbol{\Theta})], \\ &\boldsymbol{\Gamma}_{TR}(\omega) = \mathbf{I}_M \otimes \mathrm{diag}[\gamma(\omega)], \mathbf{X}_{TR} = \mathbf{I}_M \otimes \mathbf{X}, \\ &\mathbf{Z}_{TR}(\omega) = \left[\mathbf{z}_1(\omega)\mathbf{1}_M, \cdots, \mathbf{z}_M(\omega)\mathbf{1}_M\right]^T, \end{aligned} \quad (9)$$

where $\otimes$ represents Kronecker product.

3. THE PROPOSED TRF-SSMUSIC ALGORITHM

This section presents the TRF-SSMUSIC algorithm on the base of CSM method (Two-side Correlation Transformation (TCT) [9] is taken to execute the *focusing* process) and spatial-smoothing multiple signal classification (SS-MUSIC) [10, 11] from the derived TR-Echo in (8). Firstly, $\mathbf{y}_{TR}(\omega)$ is divided into Q equally spaced frequency bins. The array output vector for a fixed frequency ω_q is denoted as $\mathbf{y}_{TR}(\omega_q)$, then, the corresponding covariance matrix at the qth frequency bin can be written as

$$\Re_{\mathbf{y}}^{TR}(\omega_q) = \mathbb{E}\left\{\mathbf{y}_{TR}(\omega_q)(\mathbf{y}_{TR}(\omega_q))^H\right\}, \quad (10)$$

where $\mathbb{E}$ represents expectation operator.

The CSM method algorithm mainly transforms the signal subspaces and overlaps them in a predefined subspace: so-called *focusing* space. The problem turns into finding the transforming matrices which we denote as $\mathbf{T}_q(\omega_q)(q = 1, 2, \ldots, Q)$. In particular, TCT takes advantage of the covariance matrix at the each frequency bin to compute the transforming matrices so as to obtain the *focusing* covariance matrix $\Re_{\mathbf{y}}^{TR}(\omega_q)$. From [12, 13], we know that the transforming matrices $\mathbf{T}_q(\omega_q)$ are the solutions of the equation:

$$\mathbf{T}_q(\omega_q) \Re_{\mathbf{y}}^{TR}(\omega_q) \mathbf{T}_q^H(\omega_q) = \Re_{\mathbf{y}}^{TR}(\omega_0), \quad (11)$$

where ω_0 is the frequency of the *focusing* space. To solve (11), we convert (10) to a constrained minimization problem

$$\begin{aligned} &\min_{\mathbf{T}_q(\omega_q)} \left\| \Re_{\mathbf{y}}^{TR}(\omega_0) - \mathbf{T}_q(\omega_q) \Re_{\mathbf{y}}^{TR}(\omega_q) \mathbf{T}_q^H(\omega_q) \right\|_F, \\ &s.t.\ \mathbf{T}_q(\omega_q)^H \mathbf{T}_q(\omega_q) = \mathbf{I}, \end{aligned} \quad (12)$$

for $q = 1, 2, \ldots, Q$. In (12), symbol $\|\cdot\|$ is the Frobenius norm. Then we can get the transforming matrices $\mathbf{T}_q(\omega_q)$ at frequency bin ω_q as

$$\mathbf{T}_q(\omega_q) = \mathbf{U}(\omega_0)\mathbf{U}^H(\omega_q), \tag{13}$$

where $\mathbf{U}(\omega_0)$ and $\mathbf{U}^H(\omega_q)$ respectively denote the eigenmatrices constructed by eigenvectors of $\Re_{\mathbf{y}}^{TR}(\omega_0)$ and $\Re_{\mathbf{y}}^{TR}(\omega_q)$. Evidently, frequency of the *focusing* space ω_0 and corresponding covariance matrix $\Re_{\mathbf{y}}^{TR}(\omega_0)$ play important roles in the TCT *focusing* method. For notation simplicity, we suppress the frequency variable representing $\mathbf{T}_q(\omega_q)$ by $\mathbf{T}_q$, $\Re_{\mathbf{y}}^{TR}(\omega_q)$ by $\Re_{\mathbf{y}}^{TR}(q)$ and so on. Next, we consider how to determine ω_0. Taking the focusing error into consideration, (12) can be further replaced by

$$\begin{aligned} \varepsilon = \min_{\omega_0} \min_{\mathbf{T}_q} \left\| \Re_{\mathbf{y}}^{TR}(0) - \mathbf{T}_q \Re_{\mathbf{y}}^{TR}(q) \mathbf{T}_q^H \right\|^2, \\ s.t.\ \ \mathbf{T}_q^H \mathbf{T}_q = \mathbf{I}, q = 1, 2, \ldots, Q, \end{aligned} \tag{14}$$

where ε represents the *focusing* error of all frequency bins. From (14), when $\Re_{\mathbf{y}}^{TR}(0)$ is fixed, ε can be reformulated as

$$\begin{aligned} \varepsilon = \sum_{q=1}^{Q} \Big[&\|\Re_{\mathbf{y}}^{TR}(0)\|^2 + \|\Re_{\mathbf{y}}^{TR}(q)\|^2 \\ &-2 \sum_{p=1}^{P} \sigma_p(\Re_{\mathbf{y}}^{TR}(0)) \sigma_p(\Re_{\mathbf{y}}^{TR}(q)) \Big], \end{aligned} \tag{15}$$

where $\sigma_p(\Re_{\mathbf{y}}^{TR}(0))$ and $\sigma_p(\Re_{\mathbf{y}}^{TR}(q))$ represent the singular value of matrix $\Re_{\mathbf{y}}^{TR}(0)$, respectively. $\Re_{\mathbf{y}}^{TR}(q)$ and P is the number of non-zero singular value of them. In (13), $\Re_{\mathbf{y}}^{TR}(q)$ is not related to the *focusing* frequency ω_0, then, (15) can be modified as (16) with simple mathematical computation.

$$\min_{\omega_0} \sum_{p=1}^{P} \left[Q\sigma_p^2(\Re_{\mathbf{y}}^{TR}(0)) - 2\sigma_p(\Re_{\mathbf{y}}^{TR}(0)) \sum_{q=1}^{Q} \sigma_p(\Re_{\mathbf{y}}^{TR}(q)) \right], \tag{16}$$

The solution to (15) is given as follows (see also [12]),

$$\sigma_p(\Re_{\mathbf{y}}^{TR}(0)) = \frac{1}{Q} \sum_{q=1}^{Q} \sigma_p(\Re_{\mathbf{y}}^{TR}(q)), p = 1, 2, \ldots, P. \tag{17}$$

Evidently, (17) is the theoretical value of $\sigma_p(\Re_{\mathbf{y}}^{TR}(0))$ which cannot be obtained for the reason that the number of frequency bins is limited. Therefore, replace (17) by the following as an approximation.

$$\min_{\omega_0} \sum_{p=1}^{P} \left| \sigma_p(\Re_{\mathbf{y}}^{TR}(0)) - \frac{\mu_p}{Q} \right|^2 \text{ with } \mu_p = \sum_{q=1}^{Q} \sigma_p(\Re_{\mathbf{y}}^{TR}(q)), \tag{18}$$

Equation (18) is is a one-variable optimization problem, and a search procedure can be applied to find the minimum point so as to obtain the *focusing* frequency ω_0 conveniently. Using (18) to get the focusing frequency ω_0 and (13) to acquire transforming matrices $\mathbf{T}_q$ at each frequency bin ω_q, we can obtain the *focusing* covariance matrix $\Re_{\mathbf{y}}^{TR}(\omega_0)$ by

$$\Re_{\mathbf{y}}^{TR}(\omega_0) = \frac{1}{Q} \sum_{q=1}^{Q} \mathbf{T}_q \Re_{\mathbf{y}}^{TR}(q) \mathbf{T}_q^H. \tag{19}$$

Then SS-MUSIC algorithm can be applied on the base of (19) for DOA estimations.

Table 1. Parameters Used in the Monte Carlo Simulations

2-path	Direction of arrival	$\{2^\circ, -2^\circ\}$
	Time delays	$\{$ 0,2.3$\}$ns
	Attenuation factors	$\{1, \sqrt{1/2}\}$
3-path	Direction of arrival	$\{2^\circ, -2^\circ, -10^\circ\}$
	Time delays	$\{$ 0,2.3,11$\}$ns
	Attenuation factors	$\{1, \sqrt{1/2}, \sqrt{1/2}\}$
4-path	Direction of arrival	$\{2^\circ, -2^\circ, -10^\circ, -20^\circ\}$
	Time delays	$\{$ 0,2.3,11,22$\}$ns
	Attenuation factors	$\{1, \sqrt{1/2}, \sqrt{1/2}, \sqrt{1/2}\}$

4. NUMERICAL SIMULATIONS

In this section we conduct experiments to evaluate the DOA estimation performance using the TRF-SSMUSIC algorithm described in Section 2 and Section 3. We start by describing the parameters used in our simulations in Table 1. Two experiments are conducted to verify the proposed algorithm: i) the spatial spectra; ii) root mean squares errors (RMSE) with respect to different SNRs by the Monte Carlo simulations.

We assume a ULA consisting of $M = 16$ isotropic elements with interelement sensor space $d = \lambda_0$ with $\lambda_0 = c/f_c$, where f_c is the carrier frequency and c is is the propagation speed of the probing signal. Besides, the probing signal is assumed as a pulse with linear frequency modulation (LFM), i.e. $f(t) = \hat{f}(t)e^{jw_c t}$ where the angular carrier frequency $\omega_c = 2\pi f_c$ and the relative bandwidth is 0.1. The number of frequency bins Q is set to be 1000 (it is noted that Q has to satisfy the sampling theorem in frequency domain so as to maintain the integrity of the signal. To be more specifically, $Q \geq \tau_0 \cdot B$, see [13] for more details), which is a reasonable value for our 2-path, 3-path and 4-path propagation environments discussed below. For all of the three scenarios, the pseudospectra are plotted in Fig. 2 and performance curves in terms of RMSE versus SNRs in Fig. 3.

4.1. Spatial spectra

In this part, the simulations are based on the radar experimental setup shown in Fig. 1 with the corresponding parameters defined in Table 1. SNRs for all of the three propagation

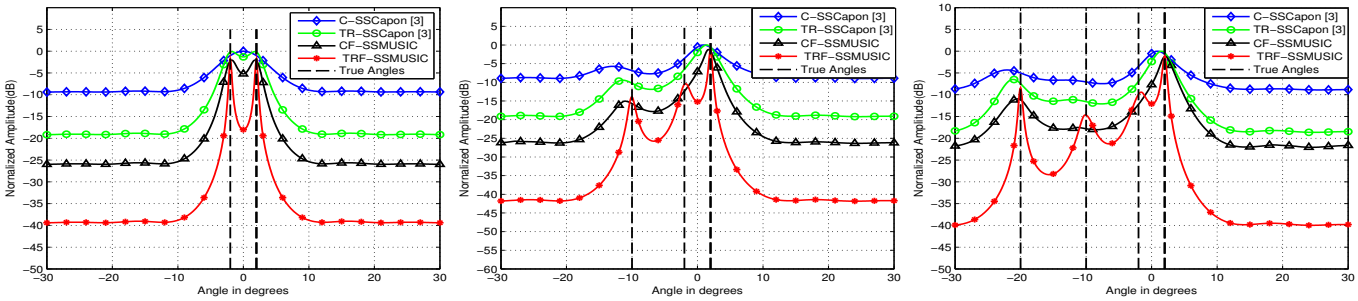

(a) 2-path (b) 3-path (c) 4-path

Fig. 2. Spectra of the four different algorithms in different propagation models: (a)2-path; (b)3-path; (c)4-path.

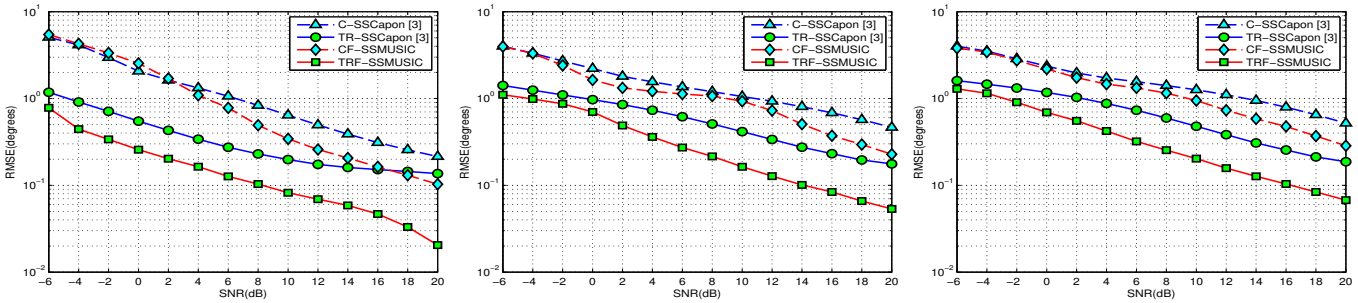

(a) 2-path (b) 3-path (c) 4-path

Fig. 3. RMSE against SNR of four different algorithms in different propagation models: (a) 2-path; (b) 3-path; (c) 4-path.

models in Fig. 2 are fixed at -5 dB. For easy reference, in Fig. 2, we plot several vertical dashed lines to denote the actual DOAs. Fig. 2 indicates that in all of the three scenarios, our proposed TRF-SSMUSIC algorithm can accurately estimate the DOAs of corresponding targets while other three algorithms (conventional spatial smoothing Capon (C-SSCapon) [3], time reversal spatial smoothing Capon (TR-SSCapon) [3], conventional *focusing* spatial smoothing MUSIC (CF-SSMUSIC)) cannot distinguish closely located targets in some conditions. Both C-SSCapon and TR-SSCapon use incoherent signal-subspace signal method (ISM [14]) to deal with the wide-band received signal. Since ISM ignores the frequency difference between every frequency bin, the performances of them degrades in some extent. Compared with CF-SSMUSIC, TRF-SSMUSIC has higher SNR and larger virtual aperture by taking time reversal technique, thus enhancing its DOA accuracy. Resolution of TRF-SSMUSIC algorithm is the best among all of the four algorithms for it has much narrower peaks in (or close to, more practically) the true DOA angles and much lower sidelobes.

4.2. RMSE versus SNR

Fig. 3 shows that RMSE for our proposed TRF-SSMUSIC algorithm has lower values than other three algorithms, that is it improves the DOA precision in a certain degree. To be more specifically, in Fig. 3(a), when the RMSE is 0.5°, the corresponding SNRs are -5 dB, 0 dB, 7 dB, 10 dB for the four algorithms, respectively. It indicates the outperformance of TRF-SSMUSIC algorithm from another aspect.

5. CONCLUSION

In this paper, a novel time reversed based DOA estimation method is proposed for low angle target scenario. TR technique and CSM method are integrated and applied to produce a new DOA estimation method. We show that matching the transmitted signal to the multipath propagation channel by TR technique improves the DOA estimation accuracy. The CSM method can accurately locate closely separated targets. In our simulations, we observe that the proposed algorithm outperforms other three conventional methods in estimation accuracy resolution and exhibits lower RMSE for a variety of SNRs. We assume time reversal waveform matches the propagation channel perfectly in this paper. In reality, however, many factors such as the noise, propagating medium and so on will lead to channel estimation errors and degrade the DOA estimation performance. Hence, further study of corresponding DOA estimation methods when existing phase error or channel mismatch remains an open research problem.

6. REFERENCES

[1] H. Krim and M. Viberg, "Two decades of array signal processing research: the parametric approach," *IEEE Signal Processing Magazine*, vol. 13, no. 4, pp. 67–94, Jul 1996.

[2] M. Fink, "Time reversal acoustics," in *Journal of Physics Conference Series*, 2008, vol. 2, pp. 850 – 859.

[3] F. Foroozan and A. Asif, "Time reversal based active array source localization," *IEEE Transactions on Signal Processing*, vol. 59, no. 6, pp. 2655–2668, June 2011.

[4] A. J. Devaney, "Time reversal imaging of obscured targets from multistatic data," *IEEE Transactions on Antennas and Propagation*, vol. 53, no. 5, pp. 1600–1610, May 2005.

[5] N. O'Donoughue and J. M. F. Moura, "Gaussian target detection in multipath clutter with single-antenna time reversal," *IEEE Transactions on Signal Processing*, vol. 61, no. 15, pp. 3733–3744, Aug 2013.

[6] W. Fan and Z. Chen, "A condition for multiple source reconstructions with the time-reversal methods," in *2016 IEEE MTT-S International Microwave Symposium (IMS)*, May 2016, pp. 1–4.

[7] H. Wang and M. Kaveh, "Coherent signal-subspace processing for the detection and estimation of angles of arrival of multiple wide-band sources," *IEEE Transactions on Acoustics, Speech, and Signal Processing*, vol. 33, no. 4, pp. 823–831, Aug 1985.

[8] F. Foroozan, A. Asif, and Y. Jin, "Cramer-rao bounds for time reversal mimo radars with multipath," *IEEE Transactions on Aerospace and Electronic Systems*, vol. 52, no. 1, pp. 137–154, February 2016.

[9] S. Valaee and P. Kabal, "Wideband array processing using a two-sided correlation transformation," *IEEE Transactions on Signal Processing*, vol. 43, no. 1, pp. 160–172, Jan 1995.

[10] R. Schmidt, "Multiple emitter location and signal parameter estimation," *IEEE Transactions on Antennas and Propagation*, vol. 34, no. 3, pp. 276–280, Mar 1986.

[11] S. Li and B. Lin, "On spatial smoothing for direction-of-arrival estimation of coherent signals in impulsive noise," in *2015 IEEE Advanced Information Technology, Electronic and Automation Control Conference (IAEAC)*, Dec 2015, pp. 339–343.

[12] R. A. Monzingo, R. L. Haupt, and T. W. Miller, *Optimum Array Processing*, IET Digital Library, 2011.

[13] P. Stoica and R. L. Moses, *Spectral Analysis of Signals*, Upper Saddle River, NJ: Prentice-Hall, 2005.

[14] M. Wax, T. Shan, and T. Kailath, "Spatio-temporal spectral analysis by eigenstructure methods," *IEEE Transactions on Acoustics, Speech, and Signal Processing*, vol. 32, no. 4, pp. 817–827, Aug 1984.